Grad-Shafranov reconstruction and Monte Carlo simulation: effects of magnetic clouds during galactic cosmic-ray Forbush decreases as observed on board LISA Pathfinder

Simone Benella[1]
Catia Grimani[1], Monica Laurenza[2], Giuseppe Consolini[2]

[1] Università degli Studi di Urbino "Carlo Bo" — DiSPeA,
Istituto Nazionale di Fisica Nucleare — Sezione di Firenze

[2] INAF — Istituto di Astrofisica e Planetologia Spaziali, Roma

INFN
2 Dicembre 2019, Sesto Fiorentino

1506 UNIVERSITÀ DEGLI STUDI DI URBINO CARLO BO

Outline

- GCR flux variability
- LISA Pathfinder mission
- Grad-Shafranov reconstruction
- Monte Carlo simulation on magnetic clouds
- The August 2, 2016 Forbush decrease on board LPF

Galactic cosmic-ray flux variability

Galactic cosmic rays

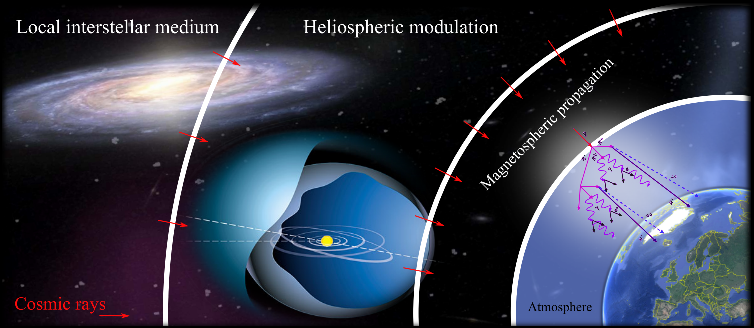

Composition

Proton 90%
Helium nuclei 8%
Electrons 1%
Heavy nuclei 1%

GCR flux variability

Long-term variations

GCR flux variations occurring over periods of time longer than one year resulting mainly correlated with the 11-year solar activity cycle and the 22-year global solar magnetic field polarity reversal. It is worthwhile to recall that the solar polarity is called positive (negative) when the solar magnetic field lines are directed outward (inward) from (to) the Sun North Pole.

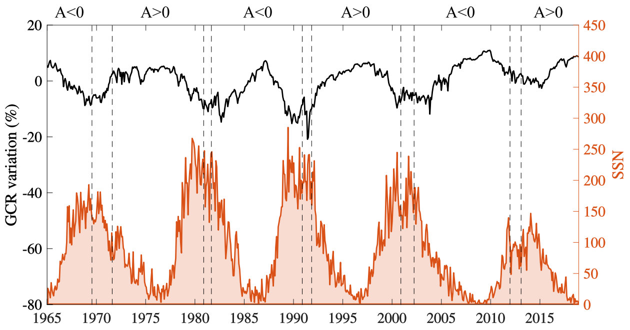

GCR flux variability

Short-term variations

GCR flux variations lasting less than one month in response to interplanetary processes such as corotating interaction regions, originated by the interaction between slow and fast solar wind streams, interplanetary coronal mass ejections (ICMEs), heliospheric current sheet crossings and others.

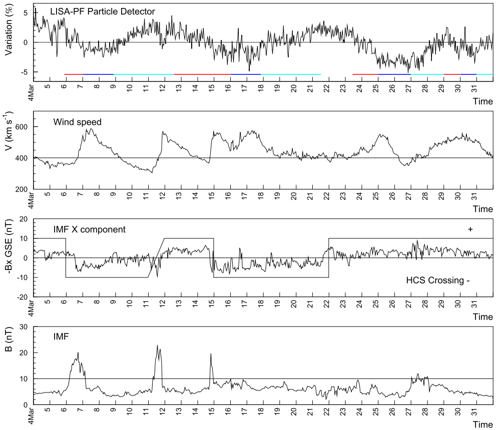

M. Armano et al., The Astrophysical Journal 854.2 (2018): 113

GCR flux short-term variations

Recurrent variations

GCR flux short-term variations associated with interplanetary disturbances originated by long-living structures on the Sun, e.g. coronal holes

Transient variations

GCR flux short-term variations originated by interaction with transient/sporadic solar wind disturbances, e.g. Interplanetary coronal mass ejections (ICMEs)

GCR recurrent short-term variations

- CIRs are regions of compressed solar wind plasma due to the interaction between slow and high speed solar wind streams
- High speed solar wind streams are originated at the Sun by coronal holes
- Periodicities related to the sun rotation period are present in GCR short-term variations

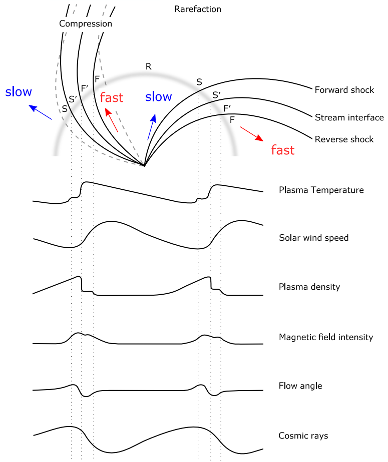

I G Richardson, Space Science Reviews, 111(3-4) :267-376 2004

GCR transient short-term variations: Forbush decreases

A Forbush decrease is a sudden drop in the observed GCR intensity due to the passage of an ICME

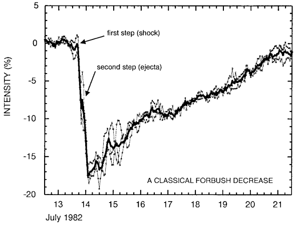

H. V. Cane, 2000, SSRv, 93, 55

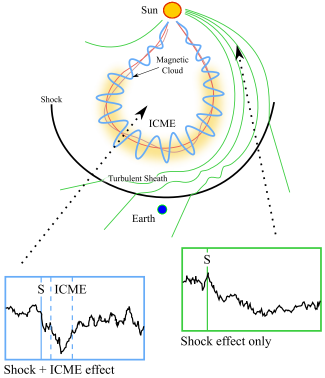

I. G. Richardson and H. V. Cane, Solar Physics 270.2 (2011) : 609-627

The LISA Pathfinder mission

LISA Pathfinder

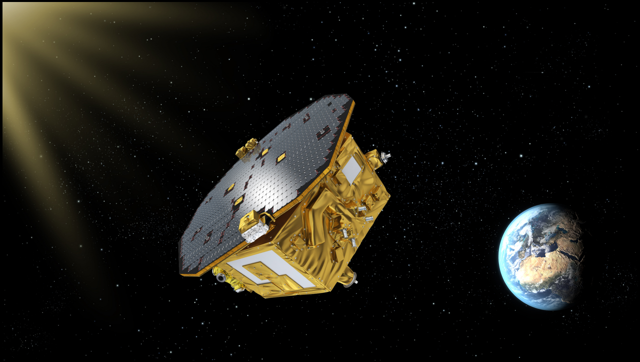

Mission launch	Dec 3, 2015
Mission end	Jul 18, 2017

LISA Pathfinder orbit

- LPF orbit was around the Earth-Sun Lagrangian point L1 at about 1.5 million km from Earth
- The orbit was inclined at about 45 degrees on the ecliptic plane
- LPF took 6 months to complete the orbit
- The satellite spinned on its own axis in 6 months

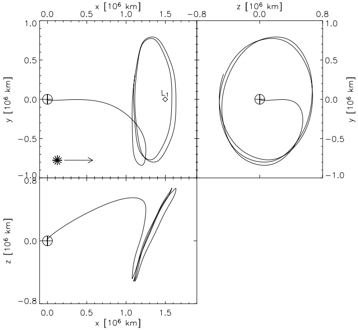

M Landgraf, et al., Classical and Quantum Gravity, 22(10) :S487, 2005

Particle Detector

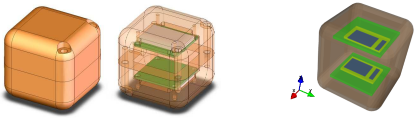

I Mateos, et al., Journal of Physics : Conference Series. Vol. 228. No. 1. IOP Publishing, 2010

Two silicon wafers 1.4x1.05x0.03 cm^3 inside a shielding copper box 6.4 mm thick

- Maximum allowed detector counting rate : 6500 counts s^{-1}
- Acquisition rate 0.067 Hz (15 counts s^{-1})
- Integral proton and helium fluxes above 70 MeV n^{-1}

Particle Detector Data

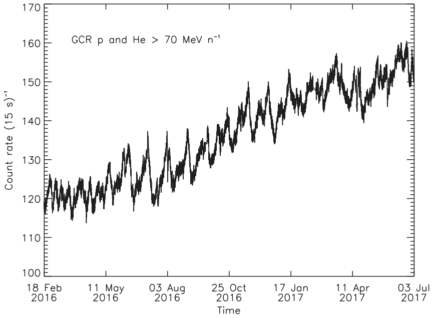

M. Armano et al., The Astrophysical Journal 854.2 (2018): 113

- LPF Particle Detector data from 2016 February 18 to 2017 July 3
- Hourly averaged data in order to limit the statistical uncertainty to 1%

Periodicity analysis: empirical mode decomposition

- No “a priori” assumptions on the basis functions
- Useful for non-linear and non-stationary datasets (Huang et al., 1998)

$$X(t) = \sum_{i=1}^{N} C_i(t) + r(t)$$

- The functions $C_i(t)$ are called Intrinsic Mode Function (IMF) and $r(t)$ is the residue of the decomposition

- Finite and small number of IMFs

N E Huang, et al., Proceedings of the Royal Society of London A : mathematical, physical and engineering sciences. Vol. 454. No. 1971. The Royal Society, 1998

G Rilling, P Flandrin, P Goncalves., IEEE-EURASIP workshop on nonlinear signal and image processing. Vol. 3. NSIP-03, Grado (I), 2003

Periodicity analysis: empirical mode decomposition

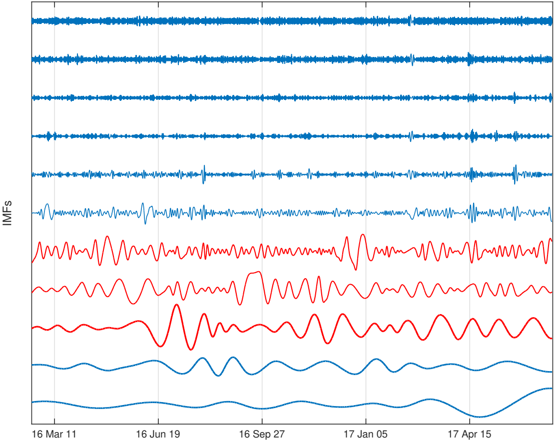

IMF#	Mean Period (days)
1	0.12 ± 0.01
2	0.21 ± 0.01
3	0.41 ± 0.01
4	0.81 ± 0.01
5	1.78 ± 0.03
6	3.8 ± 0.1
7	10.3 ± 0.3
8	14.1 ± 0.6
9	27.6 ± 1.0
10	46.3 ± 3.0
11	87.9 ± 7.1

C Grimani et al., Nuovo Cim. 42 (2019) : 42

Periodicity analysis: empirical mode decomposition

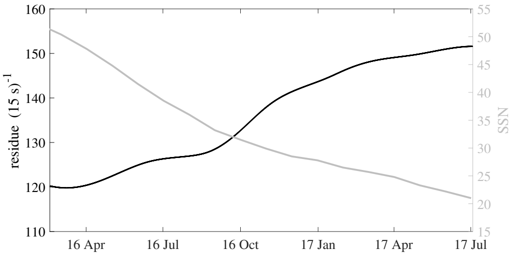

- intrinsic mode functions # 7-9 show that periodicities of 9, 13.5, and 27 days, related to the Sun rotation, are present
- the comparison between the residue of the EMD and the observed sunspot number shows that the GCR count rate presents an increasing trend over the mission lifetime due to the decreasing solar activity

S Benella et al., 36th International Cosmic Ray Conference (ICRC2019). Vol. 36. 2019

Bartels Rotation 2495 (20 Jun 2016 – 17 Jul 2016)

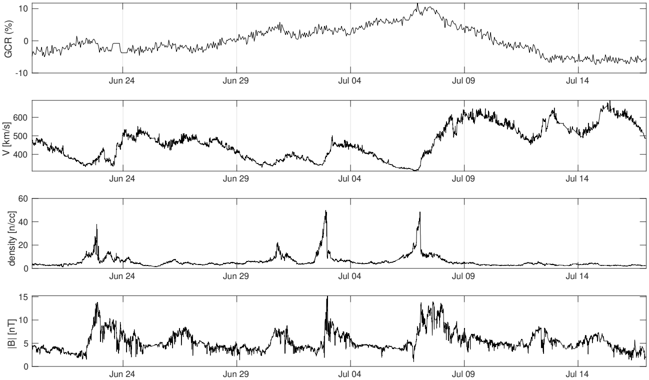

Bartels Rotation 2496 (17 Jul 2016 – 13 Aug 2016)

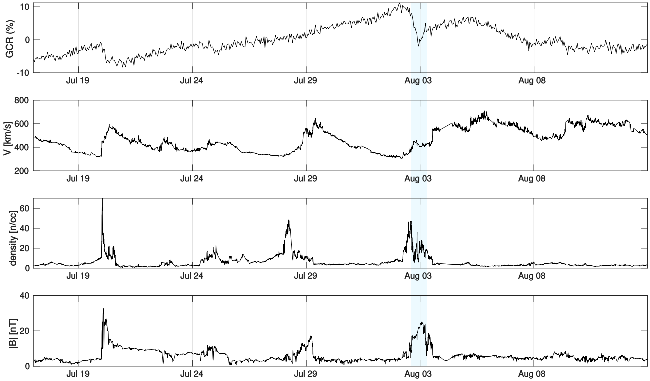

Bartels Rotation 2497 (13 Aug 2016 – 09 Sep 2016)

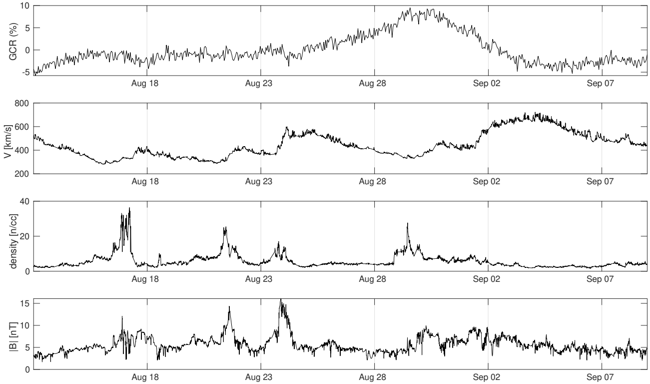

The Grad-Shafranov reconstruction

Grad-Shafranov reconstruction

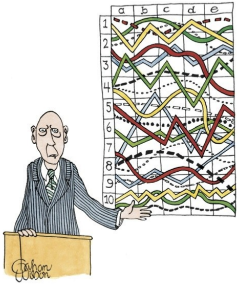

"I'll pause for a moment so you can let this information sink in."

Cartoon presented in Prof. Sonnerup's Van Allen Lecture at the 2010 AGU Fall Meeting

(New Yorker Magazine, available from http ://www.newyorker.com/cartoons/a15439)

L-N Hau, BUÖ Sonnerup, Journal of Geophysical Research: Space Physics 104.A4 (1999): 6899-6917
Q Hu, BUÖ Sonnerup, Journal of Geophysical Research: Space Physics 107.A7 (2002)
C Möstl et al., Sol. Phys. 256 (2009) 427–441

Grad-Shafranov reconstruction

- Equilibrium equation for plasma structures

$$\nabla p = \boldsymbol{j} \times \boldsymbol{B}$$

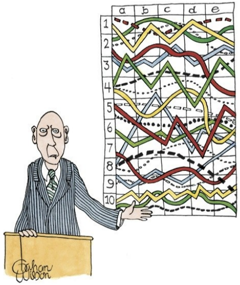

"I'll pause for a moment so you can let this information sink in."

Cartoon presented in Prof. Sonnerup's Van Allen Lecture at the 2010 AGU Fall Meeting

(New Yorker Magazine, available from http ://www.newyorker.com/cartoons/a15439)

L-N Hau, BUÖ Sonnerup, Journal of Geophysical Research: Space Physics 104.A4 (1999): 6899-6917
Q Hu, BUÖ Sonnerup, Journal of Geophysical Research: Space Physics 107.A7 (2002)
C Möstl et al., Sol. Phys. 256 (2009) 427–441

Grad-Shafranov reconstruction

- Equilibrium equation for plasma structures

$$\nabla p = \boldsymbol{j} \times \boldsymbol{B}$$

- For 2D quasi-stationary magnetic field structure, in a reference frame moving with the structure, the equilibrium equation can be written as a Grad-Shafranov (GS) plane equation (Hau and Sonnerup, 1999)

$$\frac{\partial^2 A}{\partial x^2} + \frac{\partial^2 A}{\partial y^2} = -\mu_0 \frac{d}{dA} \underbrace{\left(p + \frac{B_z^2}{2\mu_0}\right)}_{P_t}$$

where $\hat{z}$ is the invariant direction, $\partial/\partial z = 0$

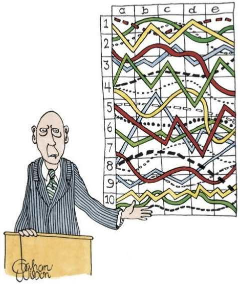

"I'll pause for a moment so you can let this information sink in."

Cartoon presented in Prof. Sonnerup's Van Allen Lecture at the 2010 AGU Fall Meeting

(New Yorker Magazine, available from http ://www.newyorker.com/cartoons/a15439)

L-N Hau, BUÖ Sonnerup, Journal of Geophysical Research: Space Physics 104.A4 (1999): 6899-6917
Q Hu, BUÖ Sonnerup, Journal of Geophysical Research: Space Physics 107.A7 (2002)
C Möstl et al., Sol. Phys. 256 (2009) 427–441

Grad-Shafranov reconstruction

- Equilibrium equation for plasma structures

$$\nabla p = \boldsymbol{j} \times \boldsymbol{B}$$

- For 2D quasi-stationary magnetic field structure, in a reference frame moving with the structure, the equilibrium equation can be written as a Grad-Shafranov (GS) plane equation (Hau and Sonnerup, 1999)

$$\frac{\partial^2 A}{\partial x^2} + \frac{\partial^2 A}{\partial y^2} = -\mu_0 \frac{d}{dA} \underbrace{\left(p + \frac{B_z^2}{2\mu_0}\right)}_{P_t}$$

where $\hat{z}$ is the invariant direction, $\partial/\partial z = 0$

- $\boldsymbol{B} = \big(\partial A/\partial y, -\partial A/\partial x, B_z(A)\big)$

L-N Hau, BUÖ Sonnerup, Journal of Geophysical Research: Space Physics 104.A4 (1999): 6899-6917
Q Hu, BUÖ Sonnerup, Journal of Geophysical Research: Space Physics 107.A7 (2002)
C Möstl et al., Sol. Phys. 256 (2009) 427–441

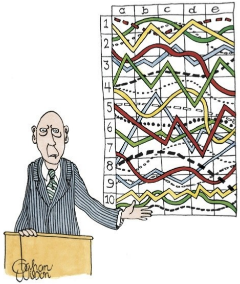

"I'll pause for a moment so you can let this information sink in."

Cartoon presented in Prof. Sonnerup's Van Allen Lecture at the 2010 AGU Fall Meeting

(New Yorker Magazine, available from http ://www.newyorker.com/cartoons/a15439)

Grad-Shafranov reconstruction

- Reference frame velocity is estimated through the de Hoffmann-Teller analysis

$$\boldsymbol{E}' = \boldsymbol{E} + \boldsymbol{V}_{HT} + \boldsymbol{B} = 0$$

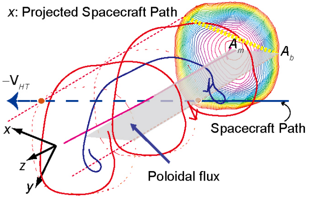

Q Hu, Science China Earth Sciences 60.8 (2017) : 1466-1494

Grad-Shafranov reconstruction

- Reference frame velocity is estimated through the de Hoffmann-Teller analysis

$$\boldsymbol{E}' = \boldsymbol{E} + \boldsymbol{V}_{HT} + \boldsymbol{B} = 0$$

- Stationarity, the Faraday's law

$$\nabla \times \boldsymbol{E}' = -\left(\frac{\partial \boldsymbol{B}}{\partial t}\right)' = 0$$

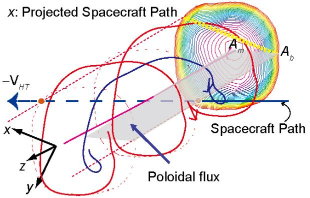

Q Hu, Science China Earth Sciences 60.8 (2017) : 1466-1494

Grad-Shafranov reconstruction

- Reference frame velocity is estimated through the de Hoffmann-Teller analysis

$$\boldsymbol{E}' = \boldsymbol{E} + \boldsymbol{V}_{HT} + \boldsymbol{B} = 0$$

- Stationarity, the Faraday's law

$$\nabla \times \boldsymbol{E}' = -\left(\frac{\partial \boldsymbol{B}}{\partial t}\right)' = 0$$

- By choosing $\hat{\boldsymbol{x}}$ along the HT velocity $-\boldsymbol{V}_{HT} \cdot \hat{\boldsymbol{x}}$ represent the projection of the S/C path

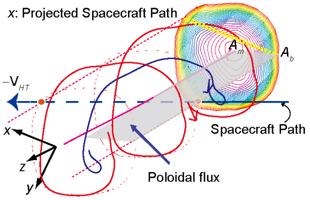

Q Hu, Science China Earth Sciences 60.8 (2017) : 1466-1494

Grad-Shafranov reconstruction

- Invariant axis estimation: first guess based on the minimum variance analysis

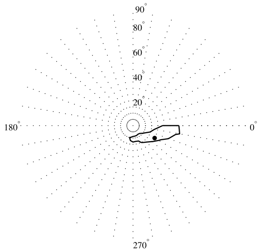

Q Hu, et al. Journal of Geophysical Research : Space Physics 109.A3 (2004)

Grad-Shafranov reconstruction

- Invariant axis estimation: first guess based on the minimum variance analysis
- Refined method based on a trial and error procedure to minimize the fit residue between the transverse pressure P_t as a function of the potential vector A only

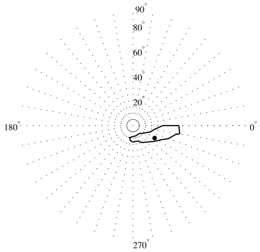

Q Hu, et al. Journal of Geophysical Research : Space Physics 109.A3 (2004)

Grad-Shafranov reconstruction

- Invariant axis estimation: first guess based on the minimum variance analysis
- Refined method based on a trial and error procedure to minimize the fit residue between the transverse pressure P_t as a function of the potential vector A only
- Calculation of the vector potential of the magnetic field $A(x, y)$ at y values distant from the S/C path placed at $y = 0$ using a second-order Taylor expansion with the GS equation

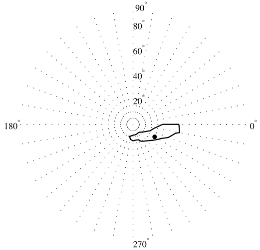

Q Hu, et al. Journal of Geophysical Research : Space Physics 109.A3 (2004)

Monte Carlo simulation

Overview

- The GS reconstruction provide a quasi-3-D magnetic map with cylindrical symmetry
- Assuming an isotropic flux outside the MC region, protons are propagated through the structure with full-trajectory integration
- After the propagation a grid is defined on the x-y plane of the GS reconstruction and the particle fluence through volume elements are computed
- The variation between the isotropic initial fluence throught the MC boundaries and the volume fluence on the grid is evaluated

Incident particle fluence

- Differential incident GCR fluence

$$F^{(in)}(E) = \int_0^{\infty} dt \, \frac{1}{\pi A} \frac{dN}{dt \, dE} = \frac{1}{\pi A} \frac{dN}{dE}$$

- If N_E particles with unit weight and energies $E \in [E, E + \Delta E]$ are injected into the simulation space through the surface $A = 2(x_{\text{max}} - x_{\text{min}})L_z + 2(y_{\text{max}} - y_{\text{min}})L_z$, where L_z is the length of the box in z direction, the total omnidirectional differential fluence at the boundaries

$$F^{(in)} = \frac{N_E}{\pi A \Delta E}$$

Volume particle fluence

- The particle distribution function $f(\boldsymbol{x}, \boldsymbol{p})$, defined as the number of particles in the position $\boldsymbol{x}$ with momentum $\boldsymbol{p}$ in the phase-space volume element $d^3x\, d^3p$, can be expressed in term of the differential flux

$$f(\boldsymbol{x}, \boldsymbol{p}) = \frac{dN}{p^2\, d^3x\, d\Omega\, dp} = \frac{v\, dN}{p^2\, d^3x\, d\Omega\, dE} = \frac{J(E)}{p^2}$$

- For an incident particle isotropic distribution the differential flux is

$$F(E) = \int_0^\infty dt\, J(E) = \int_0^\infty dt\, \frac{v}{4\pi} \frac{dN}{d^3x\, dE}$$

Volume particle fluence

- Discrete expression of the volume differential fluence

$$F_C(E) = \frac{\sum_{k=1}^{N_{C,E}} n_{C,k} v_k \Delta t}{4\pi \Delta x \Delta y L_z \Delta E}$$

  - C is the cell defined as $(x, y) \in [x_i, x_i + \Delta x] \times [y_j, y_j + \Delta y]$, where $i, j = 1, 2, \ldots M$
  - $n_{C,k}$ is the number of points of the k-th particle trajectory in the cell C
  - Δt is the Monte Carlo time step with the condition $\Delta t < \min(\Delta x, \Delta y)/c$
  - v_k is the velocity of the k-th particle

Particle fluence variation

- The differential fluence variation in the cell C as a fraction of the incident fluence is obtained combining previous equations

$$\Delta F_C(E) = \frac{F_C(E) - F^{(in)}(E)}{F^{(in)}(E)}$$

- the energy-averaged fluence variation is

$$\Delta F_C = \frac{F_C - F^{(in)}}{F^{(in)}}$$

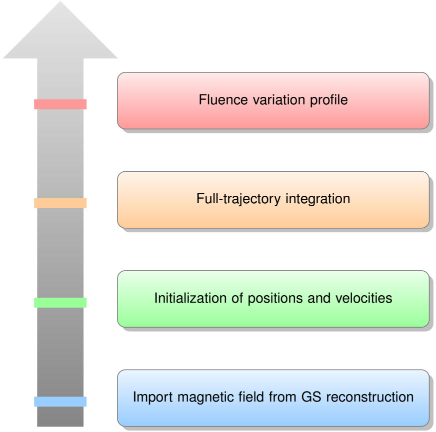

August 2, 2016 Forbush decrease

2016 Aug 2: Forbush Decrease

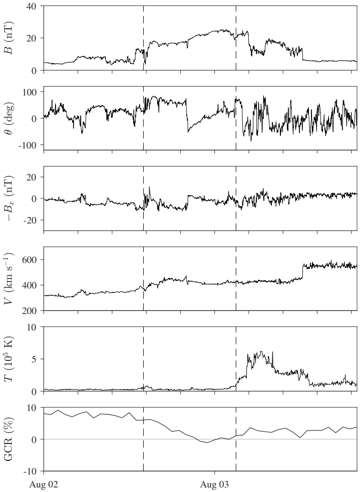

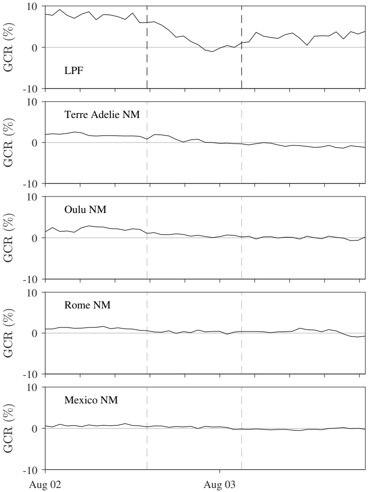

2016 Aug 2: Forbush Decrease

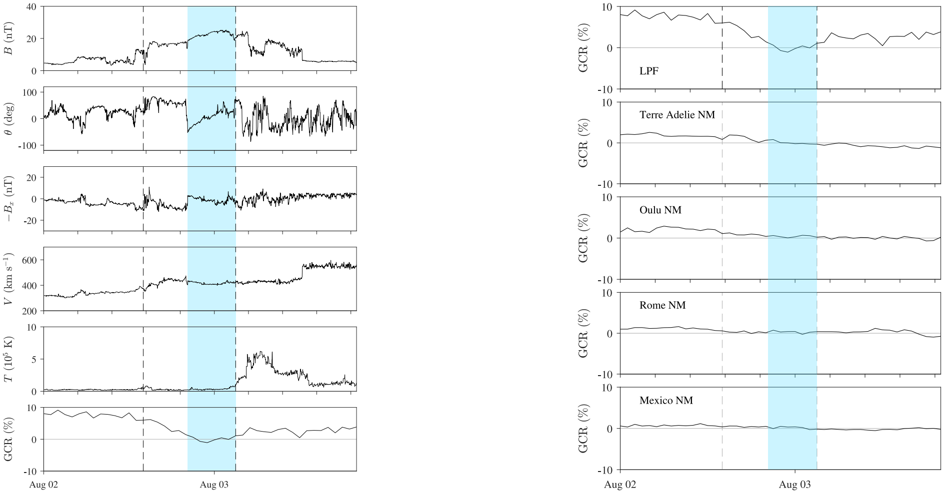

August 2, 2016 Forbush decrease

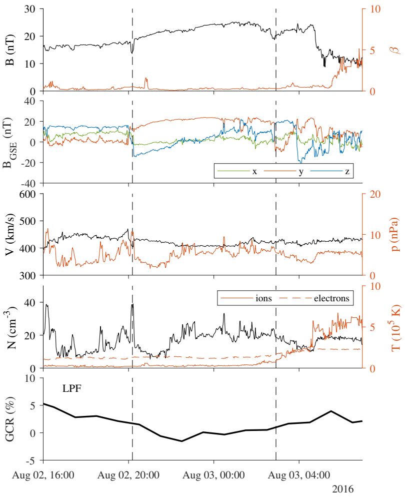

Disturbance Y/M/D (UT) (a)	ICME Plasma/Field Start, End Y/M/D (UT) (b)	
2016/08/02 1400	2016/08/02 1400	2016/08/03 0300

Richardson and Cane (http://www.srl.caltech.edu/ACE/ASC/DATA/level3/icmetable2.htm)

No.	Time Range
2683	2016/08/02 21:00 ~ 2016/08/03 02:55

Zheng and Hu (http://fluxrope.info/index.html)

- $V_{ICME} = 420$ km/s
- $V_{MAX} = 460$ km/s
- $\langle B \rangle = 22.89$ nT
- $B_{max} = 25.48$ nT

August 2, 2016 Grad-Shafranov reconstruction

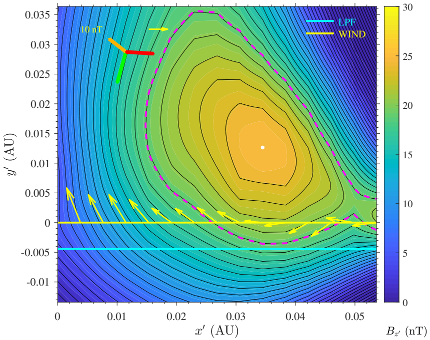

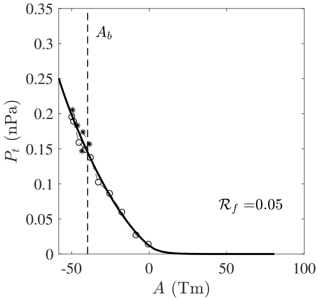

X GSE Y GSE Z GSE

- dHT velocity $[-413.69, -27.94, 11.64]$ km/s
- GS orientation: latitude $17.3 \pm 1.7°$, longitude $53.9 \pm 2.9°$
- S/C separation: $\delta y = 0.0045$ AU
- MC expansion: $|V_{exp}|/|V_{HT}| = 0.018 \ll 1$

August 2, 2016 Monte Carlo simulation

Initial proton differential energy spectrum for the August 2, 2016 event:

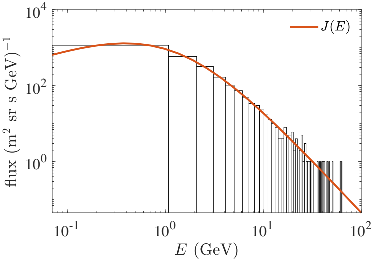

$E_{min} = 70 MeV$
$E_{max} = 100 GeV$

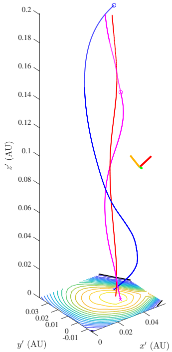

$$J(E) = A(E+b)^{-\alpha} E^{\beta}$$

$A = 18000$, $b = 1.25$, $\alpha = 3.66$ and $\beta = 0.869$

August 2, 2016 simulation results

Fluence variation matrix

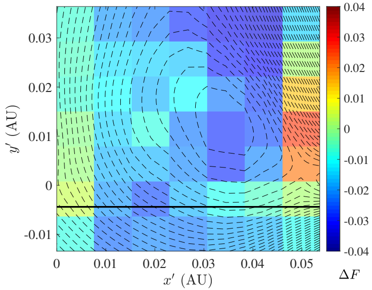

Comparison with LPF data

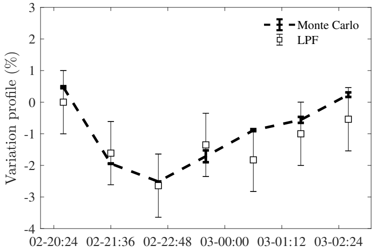

August 2, 2016 simulation results

Differential fluence variation for the August 2, 2016 Forbush decrease

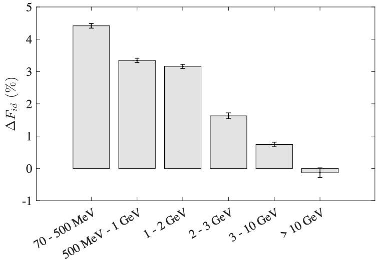

- Differential fluence variation

$$\Delta F_{id}(E) = \frac{F_i(E) - F_d(E)}{F_i(E)}$$

  - $F_i(E)$: initial omnidirectional differential fluence
  - $F_d(E)$: differential fluence in the cell associated with the dip of the FD along the LPF path

- Particles with energies > 10 GeV do not show significant variations (below 1%), thus the modulation due to the MC transit results to be uneffective
- This is confirmed by neutron monitor observations, that present an overall variation of a few percent over the whole FD event and no signature of the MC transit can be clearly detected

Conclusions

Conclusions

- Periodicities analysis is carried out using the EMD technique. Intrinsic mode functions 7-9, with mean periods of 10.3 ± 0.3, 14.1 ± 0.6 and 27.6 ± 1.0 days respectively, appear to be associated with the 27-days solar rotation period and higher harmonics. The residue of the EMD represents the data trend and is correlated with the decreasing solar activity observed during the LPF mission elapsed time.

Conclusions

- Periodicities analysis is carried out using the EMD technique. Intrinsic mode functions 7-9, with mean periods of 10.3 ± 0.3, 14.1 ± 0.6 and 27.6 ± 1.0 days respectively, appear to be associated with the 27-days solar rotation period and higher harmonics. The residue of the EMD represents the data trend and is correlated with the decreasing solar activity observed during the LPF mission elapsed time.

- The simulated particle fluence variation at the MC passage is calculated along the LPF S/C path. The amplitude of the simulated FD is found to be 3%, fully consistent with the $2.6 \pm 1\%$ observed with LPF and the time profile returned by the simulation shows an excellent agreement with the LPF data trend within error bars.

Conclusions

- Periodicities analysis is carried out using the EMD technique. Intrinsic mode functions 7-9, with mean periods of 10.3 ± 0.3, 14.1 ± 0.6 and 27.6 ± 1.0 days respectively, appear to be associated with the 27-days solar rotation period and higher harmonics. The residue of the EMD represents the data trend and is correlated with the decreasing solar activity observed during the LPF mission elapsed time.

- The simulated particle fluence variation at the MC passage is calculated along the LPF S/C path. The amplitude of the simulated FD is found to be 3%, fully consistent with the 2.6 ± 1% observed with LPF and the time profile returned by the simulation shows an excellent agreement with the LPF data trend within error bars.

- The diffusion of particles perpendicularly to the mean magnetic field includes two processes : 1) field line crossings due to scattering or drift and 2) random walk along field lines. The only mechanisms included in our simulation are gradient and curvature drifts. The excellent agreement between the LPF observations gathered during the MC transit and the Monte Carlo simulation outcome shows that for this case the random-walk-like diffusion gives a negligible contribution to the MC-driven GCR FD observed in space.

Thank you for your attention !

Questions ?